

Compositional effects on the formation of a calcium phosphate layer and the response of osteoblast-like cells on polymer-bioactive glass composites

Helen H. Lu^{*}, Amy Tang, Seong Cheol Oh, Jeffrey P. Spalazzi, Kathie Dionisio

Biomaterials and Interface Tissue Engineering Laboratory, Department of Biomedical Engineering, Columbia University, 351 Engineering Terrace Building, MC 8904, 1210 Amsterdam Avenue, New York, NY 10027, USA

Received 20 October 2004; accepted 12 April 2005
Available online 24 May 2005

Abstract

Biodegradable polymer-ceramic composites are attractive systems for bone tissue engineering applications. These composites have the combined advantages of the component phases, as well as the inherent ease in optimization where desired material properties can be tailored in a well-controlled manner. This study focuses on the optimization of a polylactide-*co*-glycolide (PLAGA) and 45S5 bioactive glass (BG) composite for bone tissue engineering. The first objective is to examine the effects of composition or overall BG content on the formation of a Ca–P layer on the PLAGA–BG composite. It is expected that with increasing BG content (0%, 10%, 25%, 50% by weight), the required incubation time in a simulated body fluid (SBF) for the composite to form a detectable surface Ca–P layer will decrease. Both the kinetics and the chemistry will be determined using SEM + EDAX, FTIR, and μ -CT methods. Solution phosphorous and calcium concentrations will also be measured. The second objective of the study is to determine the effects of BG content on the maturation of osteoblast-like cells on the PLAGA–BG composite. It is hypothesized that mineralization will increase with increasing BG content, and the composite will support the proliferation and differentiation of osteoblasts. Specifically, cell proliferation, alkaline phosphatase activity and mineralization will be monitored as a function of BG content (0%, 10%, 50% by weight) and culturing time. It was found that the kinetics of Ca–P layer formation and the resulting Ca–P chemistry were dependent on BG content. The response of human osteoblast-like cells to the PLAGA–BG composite was also a function of BG content. The 10% and 25% BG composite supported greater osteoblast growth and differentiation compared to the 50% BG group. The results of this study suggest that there is a threshold BG content which is optimal for osteoblast growth, and the interactions between PLAGA and BG may modulate the kinetics of Ca–P formation and the overall cellular response.

© 2005 Elsevier Ltd. All rights reserved.

Keywords: Polymer-ceramic composite; Bioactivity; Degradable polymers; Bioactive glass; Osteoblasts; Mineralization

1. Introduction

Orthopedic implants constitute over 50% of all implantation procedures performed in the United States, and bone is the most often replaced organ of the body, with over 500,000 bone repair procedures surgeries performed annually [1]. Clinically, both

biological and synthetic grafts have been utilized for bone repair. The preferred grafts of choice are autografts harvested from the iliac crest which have a success rate of 80–90% with minimal risk of immune rejection, infection, or disease transfer [2]. However, autografts are limited in supply, restricted by anatomical incompatibilities, and are associated with donor site morbidity. These limitations have prompted significant interest in alternatives such as tissue-engineered grafts. Tissue-engineered bone grafts are attractive because they can be designed to exhibit many advantages of autografts,

^{*}Corresponding author. Tel.: +1 212 854 4071; fax: +1 212 854 8725.

E-mail address: hl2052@columbia.edu (H.H. Lu).

without the aforementioned limitations. First, since these grafts are populated with autogenous cells, the issue of graft rejection is obviated. Second, with the addition of appropriate growth factors, the grafts can be engineered to be osteoinductive. Lastly, by utilizing a biomaterial substrate whose physical and structural properties mimic those of biological bone, an osteoconductive and osteointegrative construct can be engineered.

Material selection is a critical parameter in bone tissue engineering. A supporting scaffold is essential for maintaining mechanical strength, structural support, and for providing the optimal growth environment for bone formation during the early stages of the repair process [3–6]. Since no single existing material possesses all the necessary properties required for an ideal bone graft, there is a growing interest in the development of composite materials. The promise of combined advantages of the composite phases, as well as the inherent ease in optimization where desired material properties can be accentuated in a well-controlled manner, have made composites attractive for biomedical applications. From a biomimetic standpoint, various types of biological tissue such as bone are composite tissues with organic and inorganic phases, various cell types, extracellular matrix and bone mineral.

Several groups have begun to explore the potential of combining bioactive glass (BG) and polymers to form composite materials for bone tissue engineering [7–13]. The type of polymer–BG composite under research for bone repair has been predominantly particle-reinforced, with the exception of Marcolongo et al. [11] who implanted composite rods of polysulfone and BG fibers in rabbit femora. We recently combined polylactide-*co*-glycolide (PLAGA) 50:50 and 45S5 BG to engineer a degradable, three-dimensional composite (PLAGA–BG) scaffold [8]. The advantages of PLAGA are its documented biocompatibility, degradability, and relative ease of fabrication. However, PLAGA alone often does not have the necessary mechanical strength required for loading, lacks the ability to integrate with bone, and releases acidic degradation products which can have adverse effects on tissue response. BG was developed by Hench et al. [14,15] in the early 1970s, and it remains the most bone-bioactive material known to date [16–18]. Its bioactivity or osteointegration potential is directly related to the formation of a surface calcium phosphate (Ca–P) layer [19,20]. The biocompatibility, osteoconductivity, and osteoinductivity of BG have been well documented [19,21–26]. As such, the direct application of BG in load-bearing applications has been limited because BG is brittle and exhibits poor tensile and torsional properties [21,27,28].

The PLAGA–BG composite [8] was designed to integrate the advantages of the parent phases, while minimizing known limitations associated with each

component. A significant advantage of PLAGA–BG over PLAGA is its osteointegration potential or the ability to form a surface Ca–P layer *in vitro*. Osteointegration is a critical factor in facilitating the chemical fixation of a biomaterial to bone tissue. The second advantage of the composite is that the addition of BG to the PLAGA matrix results in a structure with a higher compressive modulus than PLAGA alone. A successful tissue-engineered scaffold must exhibit mechanical properties similar to those of the tissue to be replaced, and the compressive strength and modulus of the composite do approach those of trabecular bone. Therefore, the PLAGA–BG composite would render greater functionality *in vivo* compared to the PLAGA alone. Moreover, the combination of the two phases serves to neutralize both the acidic byproducts produced during polymer degradation and the alkalinity due to the formation of the calcium phosphate layer [8]. Through hydrolysis reactions, PLAGA degrades into glycolic and lactic acids, the release of which can induce a biologically significant decrease in local pH. For BG to bond to bone, a surface Ca–P layer is formed through a series of dissolution, precipitation and ion exchange reactions which result in an elevated local pH due to the release of alkaline ions such as Si, Na, Ca and P. By combining PLAGA and BG, the acidic and basic degradation products are neutralized, a physiological pH is maintained and the composite supports the growth and differentiation of human osteoblast-like cells *in vitro* [8].

While significant progress has been made in the formation of PLAGA–BG composites, there is still a limited understanding of the interactions between the component phases of the composite, and a lack of insight into the design rules, which govern the extended functionality of this type of scaffold. It is critical that the kinetics of osteointegration, degradation, and new bone formation are precisely engineered such that the system is functional clinically. In order to optimize the PLAGA–BG composite for bone tissue engineering, the objectives of this study are two-fold. The first aim is to examine the effects of BG content on the formation of a Ca–P layer on the PLAGA–BG composite. It is expected that with increasing BG content, the required incubation time in a simulated body fluid (SBF) for the formation of a detectable Ca–P layer will decrease. Both the kinetics and the chemistry of the Ca–P layer will be examined. The second study aim is to determine the effects of BG content on the maturation of osteoblast-like cells on the PLAGA–BG composite. It is hypothesized that mineralization will increase with increasing BG content, and the composite will support the proliferation and differentiation of osteoblasts. Specifically, cell proliferation, alkaline phosphatase (ALP) activity and mineralization will be monitored as a function of BG content and culturing time.

Findings from these studies will augment current understanding of the mechanism of bioactivity modulating the osteointegration potential of PLAGA–BG composites. They will also facilitate the identification of a suitable combination of PLAGA with BG, which will result in a biocompatible, osteointegrative and osteoconductive composite.

2. Materials and methods

2.1. Fabrication of PLAGA–BG composite

Poly(lactide-co-glycolide) 85:15 co-polymer (PLAGA, Purasorb PDLG, inherent viscosity = 3.42 dl g^{-1} , PURAC Biochem, Netherlands) and 45S5 BG (MO-SCI Corporation, Rolla, MO) granules were used to fabricate the composite (PLAGA–BG) disks. The composition of BG was 45.0% SiO_2 , 24.4% Na_2O , 24.6% CaO , and 6.0% P_2O_5 by weight. PLAGA–BG composites with varying concentrations of BG (0%, 10%, 25%, 50% BG by weight) were prepared following the traditional solvent-casting process [8]. Briefly, PLAGA and BG granules ($<40 \mu\text{m}$) were first mixed according to the polymer to ceramic weight ratio, and then dissolved in methylene chloride. The suspension was poured into a custom mold and cooled overnight at -20°C to form a PLAGA–BG film. To examine Ca–P layer formation, the composite films were bored into 10 mm diameter and 0.1-mm-thick disks. For the osteoblast studies, the samples were sectioned into $7.87 \times 7.87 \text{ mm} \times 0.1 \text{ mm}$ squares using a custom-made grid.

2.2. Compositional effects on the formation of Ca–P layer on the PLAGA–BG composite

2.2.1. Incubation in a simulated body fluid (SBF)

The development of a surface Ca–P layer on the PLAGA–BG composites was evaluated in an SBF with solution ion concentrations similar to those of blood plasma [29]. The calculated ion concentrations of the SBF were as follows: 163.4 mM Na^+ , 149.8 mM Cl^- , 2.5 mM Ca^{2+} , 28.2 mM HCO_3^- , 1.45 mM Mg^{2+} , 0.84 mM SO_4^{2-} , and 1.0 mM HPO_4^- . PLAGA–BG disks ($n = 8$) with 0%, 10%, 25% and 50% BG content were incubated at 37°C in SBF for 1, 3, 7, 14, 21, and 28 days. A surface area to volume ratio of 0.1 cm^{-1} was maintained for all immersions [19].

For the 50% BG group, the effect of solution exchange on the kinetics of Ca–P formation was determined by controlling the frequency of solution exchange during the 4-week period. In the *static mode*, with the 0.1 cm^{-1} surface area to volume ratio and assuming perfect-sink conditions, the solution was not exchanged during the experiment. The SBF solution

without any PLAGA or PLAGA–BG composites served as the control group. In the *dynamic mode*, 50% of the solution for each sample was exchanged every other day in order to mimic the physiological environment and to avoid forming a phosphate concentration gradient.

2.2.2. Characterization of Ca–P layer and solution ion concentration

The formation and elemental composition of the surface Ca–P layer developed on the samples were characterized using scanning electron microscopy (SEM, JEOL-5600LV, Tokyo, Japan) coupled with Energy Dispersive X-ray Analysis (EDAX, Phoenix Pro, EDAX, Mahwah, NJ), respectively. The samples were dehydrated using an ethanol series, and were pre-coated with carbon in order to minimize charging effects. The chemistry of the formed Ca–P layer was examined using Fourier transform infrared spectroscopy (FTIR, FTS 3000MX Excalibur Series, Digilab, Randolph, MA). The samples were dried in a chemical hood, and FTIR spectra were collected in diffuse reflectance mode (400 scans, resolution at 4 cm^{-1}). The distribution of Ca–P on the composite was evaluated using micro-computer tomography ($\mu\text{-CT}$, $\mu\text{CT} 20$, SCANCO Medical, Bassersdorf, Switzerland) following the methods of Lin et al. [30].

Solution pH was monitored over time, reflecting the balance between ion dissolution from BG during Ca–P formation and the release of degradation products from PLAGA. The concentration of phosphorous ([P], $n = 8$), the limiting factor in the mineralization process, was measured using a colorimetric assay [31]. In addition, the solution calcium concentration ([Ca], $n = 8$) was measured using a commercially available calcium kit (Pointe Scientific, Inc., Lincoln Park, MI). This colorimetric [Ca] assay was performed by following the manufacturer's protocol, and a standard curve based on a relevant range of [Ca] was generated. Absorbance was determined at 405 nm for [P] and 620 nm for [Ca] (Tecan, Maennedorf, Switzerland). Ion concentrations were calculated based on the standard curves.

2.3. Compositional effects on the response of osteoblasts on PLAGA–BG composites

2.3.1. Culture of SaOS-2 cells on PLAGA–BG composites

Human osteosarcoma cells (SaOS-2, ATCC#HTB-85) were cultured in Dulbecco's Modified Eagles Medium, supplemented with 10% fetal bovine serum, L-glutamine, 1.0 volume% non-essential amino acids, and 1.0 volume% antibiotics (all solutions and chemicals were purchased from Mediatech, Herdon, VA). The cells were grown to confluence at 37°C and 5% CO_2 . To evaluate the effect of PLAGA–BG composition on osteoblasts, SaOS-2 cells were seeded on the

PLAGA–BG composite disks (0%, 10%, 50% BG) at a density of 5×10^4 cells/cm². The samples were cultured in 24-well plates for 1, 3, 7, 14, 21, and 28 days. Mineralization medium containing 3.0 mM β -glycerophosphate and 10 μ g ml⁻¹ L-ascorbic acid (both from Sigma, St. Louis, MO) were added to the cultures at day 7.

2.3.2. SaOS-2 cell growth and differentiation on PLAGA–BG composites

Cell growth morphology on the composite was assessed by SEM (5 kV, JEOL 5600-LV, Tokyo, Japan). At the designated time points, the samples were washed three times with phosphate buffer saline in order to remove unattached cells. For SEM analysis, the samples were fixed overnight in Karnovsky's fixative and dehydrated using an ethanol series. Cell proliferation ($n = 6$) was quantified using the Picogreen dsDNA Quantitation assay (Molecular Probes, Eugene, OR). Following the manufacturer's protocols, fluorescence at 535 nm was measured (Tecan, Maennedorf, Switzerland), and its intensity was correlated to DNA concentration.

The ALP activity of SaOS-2 cells was assessed using both quantitative and qualitative assays. For the colorimetric ALP assay, the samples ($n = 6$) were first incubated at 37 °C for 30 min in 0.1 M Na₂CO₃ buffer containing 2 mM MgCl₂ with disodium *p*-nitrophenyl phosphate (*p*NP-PO₄) as the substrate. Absorbance was measured at 405 nm (Tecan, Maennedorf, Switzerland). Enzymatic activity was then expressed as total nanomoles of pNP produced per minute per total cell number. ALP visualization was performed via staining by Fast Blue RR Salt (Sigma, St. Louis, MO) in deionized water, and then diluting the solution with the Naphthol AS-MX Phosphate Alkaline Solution (Sigma, St. Louis, MO). Samples were fixed with neutral buffered formalin, incubated in the ALP staining solution for 30 min and washed with DI water before imaging (Axiovert 25C, Carl Zeiss, Germany). Alizarin Red S (ALZ) assay staining specific for calcium was used for mineralization. The samples were washed in ddH₂O and incubated in 40 mM ALZ solution for 10 min. After washing in ddH₂O, the samples were imaged by light microscopy (Axiovert 25C, Carl Zeiss, Germany).

2.4. Statistical analysis

Data in the graphs are presented in the form of mean \pm standard deviation (Mean \pm SD), with n equal to the number of samples. In the case of multiple comparisons, one-way and two-way analyses of variance (ANOVA) were performed (JMP IN[®], SAS Institute, Cary, NC), and the Tukey-Kramer test was used to

compare between the means. Significance was attained at $p < 0.05$.

3. Results

3.1. Compositional effects on the formation of Ca–P layer on the PLAGA–BG composites

3.1.1. Characterization of the surface Ca–P layer

The effects of BG content on Ca–P layer formation and distribution were examined in SBF over a four-week period. The rate of Ca–P formation on PLAGA–BG was dependent on BG content. With increasing BG content, incubation time required for the formation of Ca–P nodules decreased. Micro-CT analysis revealed that compared to the 0% BG, the 10%, 25%, and 50% BG composite formed a Ca–P layer after 7 days in SBF. At day 0, the detectable mineralized region (black regions, Fig. 1a) represented only 0.768% of the disc area. The light and light grey areas correspond to PLAGA–BG, while the outer ring corresponds to the plastic specimen holder. At day 28, the mineralized region made up 32.9% of the total area. SEM analysis (Fig. 1b) revealed abundant Ca–P deposition on the 50% BG samples after 7 days, while characteristic degradation-related surface pores were observed on the 0% control. The size of Ca–P nodules and the overall surface coverage visibly increased as immersion continued.

The chemistry and surface composition of the PLAGA–BG composite over time was analyzed for the substrates immersed in SBF. Fig. 2 compares the elemental compositions of the 0%, 10% and 50% BG composite surfaces after 14 days of immersion in the SBF. The PLAGA control surface did not mineralize and was comprised mostly of carbon and oxygen, which were characteristic of the PLAGA substrate. In contrast, EDAX analysis of the composite disks revealed the presence of Ca and P, as well as Si and Na, which were distinctive components of the BG phase. The peak intensities and peak-to-peak ratios differed between the substrates, with a relative higher intensity of Si and Na found on the 10% BG compared to the 50% BG composite. In addition, Cl and Mg were detected on the 50% BG surface, likely due to precipitation of these ions from the SBF. The Ca/P peak intensity ratio on the 10% BG surface was found to be greater than that of the 50% BG composite, and differed from the stoichiometric Ca/P ratio of 1.67 expected for hydroxyapatite.

FTIR was used to monitor the formation and growth of the Ca–P layer on PLAGA–BG by detecting characteristic vibration modes of the P–O and P = O bonds. Fig. 3 compares the FTIR spectra of the PLAGA control (0% BG) with those of the PLAGA–BG group (50% BG) at days 0 and 21. Of interest here is

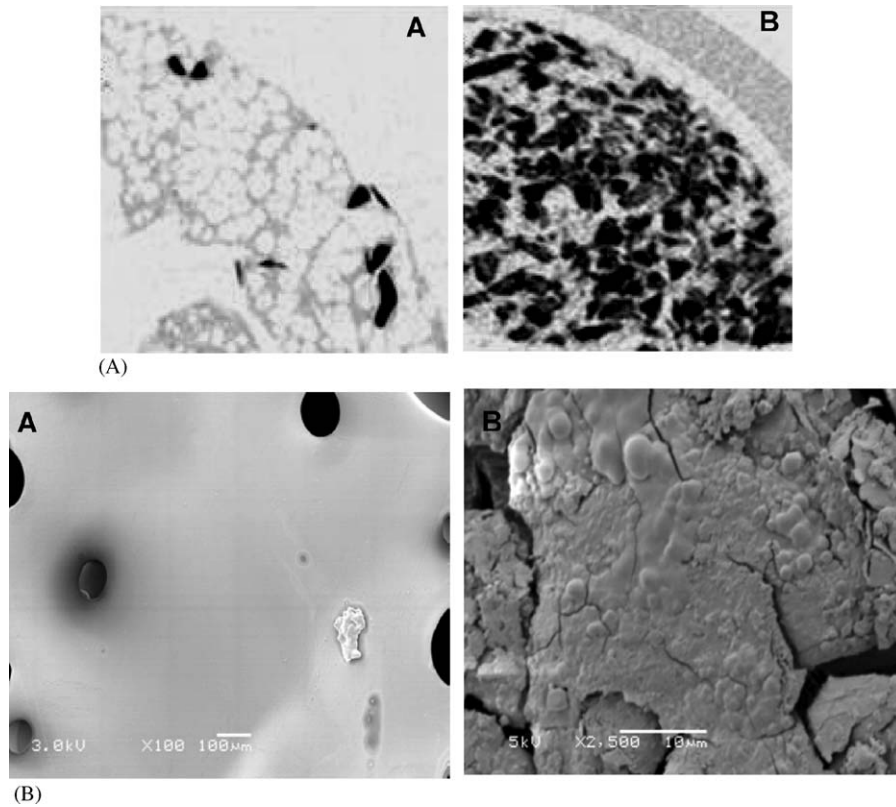


Fig. 1. Effects of composition on the formation of a surface calcium phosphate (Ca-P) layer on polymer-bioactive glass composite (PLAGA-BG). Compared to PLAGA controls (0% BG), the PLAGA-BG composite formed a surface Ca-P layer after 7 days. The size of Ca-P nodules grew and the overall surface coverage visibly increased as immersion continued. (a) Micro-CT images of PLAGA-BG after immersion in SBF, showing calcium phosphate distribution (dark phase) on 25% BG composite at (A) day 0, (B) day 28. (b) SEM micrographs of (A) 0% and (B) 50% BG surfaces after 7 days in SBF. Note the abundant deposition of Ca-P on the 50% samples, while characteristic polymer degradation related pores were observed on the 0% group.

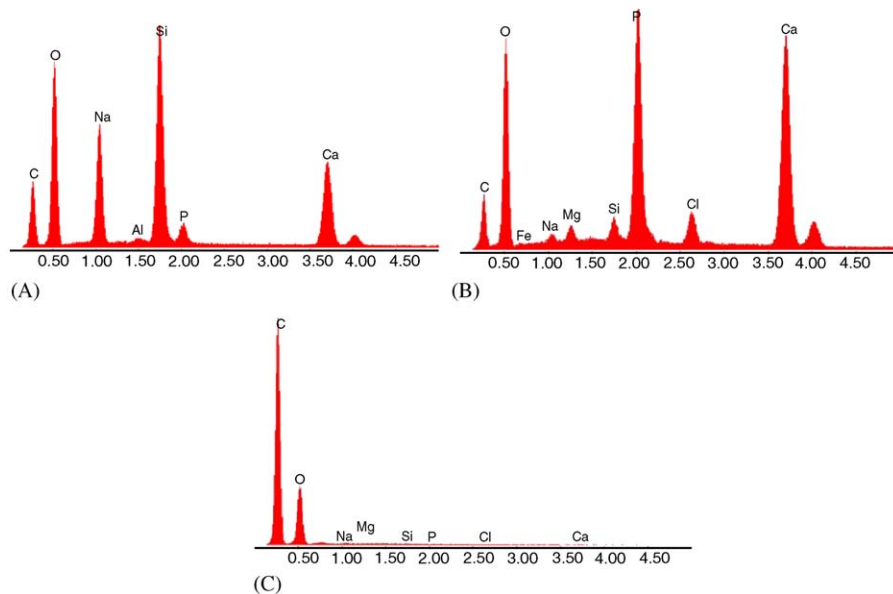


Fig. 2. Elemental analyses of the PLAGA-BG (10% and 50%, A and B, respectively) and PLAGA control (0%, C) surfaces after 14 days of immersion. EDAX analyses revealed the presence of Ca and P, as well as Si and Na, which are characteristic components of the BG phase. Surface elemental composition was dependent on the amount of BG present, with a faster leaching of Si and Na from the composite at higher BG content. Interestingly, the chemistry of the Ca-P seems to be dependent on the BG content in the composite, as Ca/P peak intensity ratio differs between 10% and 50% BG groups.

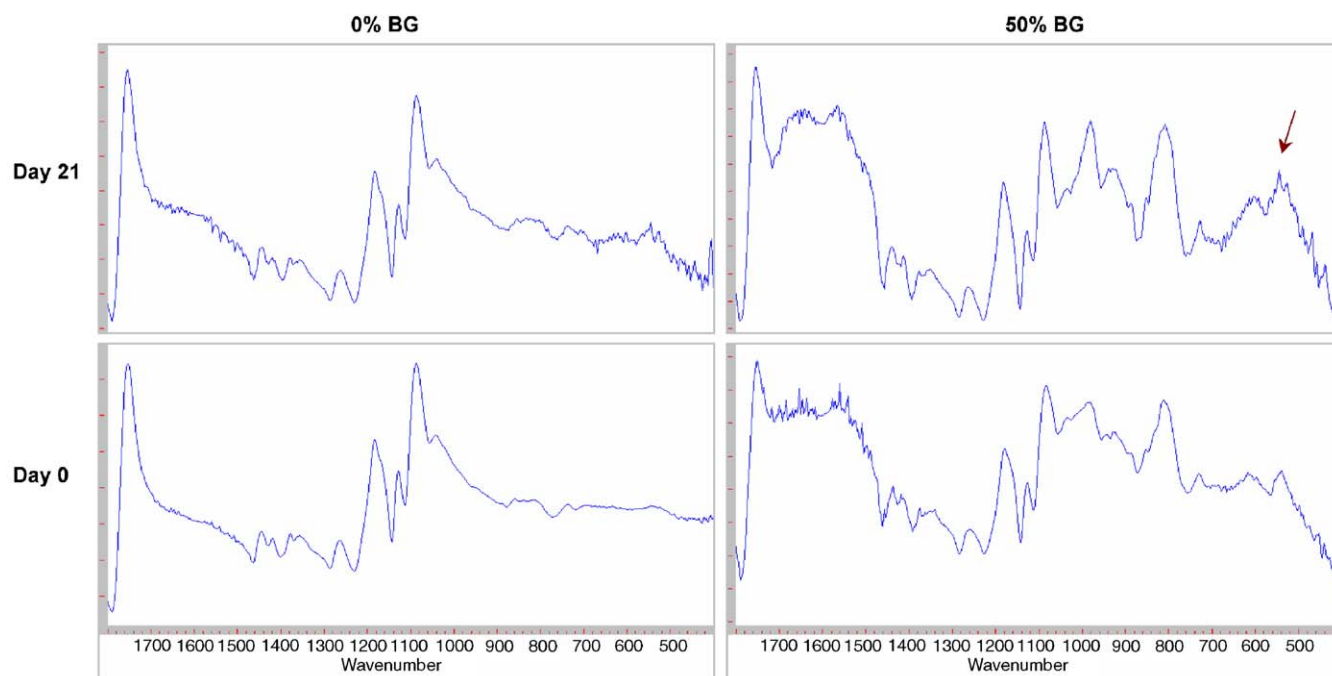


Fig. 3. FTIR spectra of PLAGA control (0%) and PLAGA–BG (50%) surfaces at day 0 and after 21 days of immersion in SBF. Characteristic peaks of PLAGA are located at 1755 and 1455 cm^{-1} , with a C–O stretch at 1091 cm^{-1} . A crystalline calcium phosphate layer was formed on the surface of the composite discs by day 21, as indicated by a split P–O bending vibration peak between 600 and 500 cm^{-1} (arrow). Peaks indicative of this calcium phosphate layer were at background levels in the PLAGA control. Spectra are represented in % transmittance.

the appearance of a P–O bending vibrational band between 600 and 570 cm^{-1} , indicative of the presence of amorphous calcium phosphate on the surface [19,29]. The characteristic FTIR peaks associated with poly α -hydroxyesters [32] or PLAGA are located at 1755 and 1455 cm^{-1} , with a C–O stretch at 1091 cm^{-1} . These peaks were observed in the spectra for the PLAGA control and the PLAGA–BG composite groups. The polymer-associated peaks also remained relatively unchanged over time. FTIR analysis of the composite surfaces immersed in SBF confirmed that a Ca–P layer was formed on PLAGA–BG as a function of time and BG content. An amorphous Ca–P layer was formed on the 25% BG discs after 14 days, while no such layer was found on the 0% BG. As seen in Fig. 3, at day 21, a crystalline Ca–P layer was detected on the 50% BG surface, as indicated by the divided P–O bending vibration peak between 600 and 500 cm^{-1} . This peak was not observed for the 0% BG controls.

3.1.2. Solution analyses and effects of solution exchange

Solution pH was monitored closely during the immersion process. As shown in Fig. 4a, the pH of the sample solutions stayed within the physiological range, and varied between 7.4 and 7.7 for the length of the experiment. With increasing BG content, a larger pH increase was observed. While the magnitude was still within the physiological range, pH for the 50% BG group was significantly higher ($p < 0.05$) compared to all

other groups tested. Solution pH in the dynamic mode (Fig. 4a) was closer to the physiological range compared to pH in the static mode (data not shown) where no media was exchanged over time.

Solution ion concentration as a function of time and BG content under both dynamic and static immersions are presented in Figs. 4b ($[\text{P}]_{\text{dynamic}}$), Fig. 5a ($[\text{P}]_{\text{static}}$), and Fig. 5b ($[\text{Ca}]_{\text{static}}$). Phosphate concentration was found to be dependent on both composition and the mode of media exchange. When SBF was exchanged regularly in the dynamic mode (Fig. 4b), $[\text{P}]_{\text{dynamic}}$ increased during the first 14 days of immersion for all groups tested, likely due to the natural fluctuations of the SBF solution with the addition of the composite. The increase in $[\text{P}]_{\text{dynamic}}$ was not significantly different for the 0% BG or the 50% BG groups during the first 2 weeks, while a significant release was measured for the 25% group at day 14. After day 14, $[\text{P}]_{\text{dynamic}}$ decreased over time and at day 21, it was significantly lower for the 25% BG and 50% BG content groups compared to PLAGA control (0% BG), suggesting that a larger precipitation of phosphate ions was associated with increased BG content over time. While the variations in ion concentration were higher than those of SBF alone, the changes in $[\text{P}]_{\text{dynamic}}$ for the 0% BG control were not statistically significant over time.

In contrast, when the 50% BG samples were immersed in the static mode during which no media exchange was performed, the total cumulative $[\text{P}]_{\text{static}}$

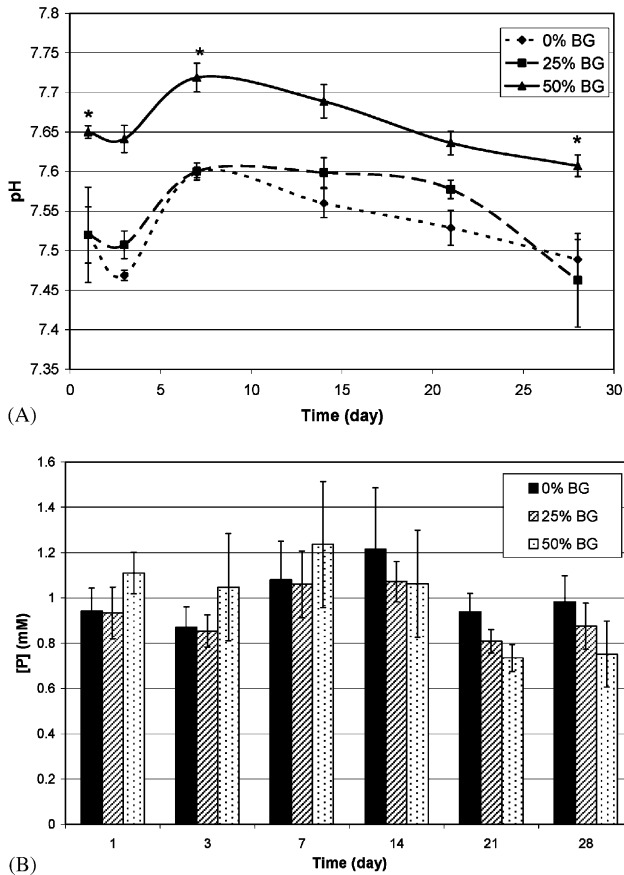


Fig. 4. Effects of composition on the mechanism of surface calcium phosphate layer (Ca-P) formation on polymer–bioactive glass composite (PLAGA–BG). As expected, solution alkalinity increased with increasing BG content. The presence of PLAGA buffered the potential increase in solution pH due to ion dissolution from BG. The concentration of phosphorus [P] decreased over time and with greater precipitation associated with 50% BG. These results suggest that ion precipitation is one of the mechanisms driving the formation of the Ca–P layer on the PLAGA–BG composite. (a) Solution pH changes ($n = 8$) over time as a function of composite BG content. (b) Solution phosphorus concentration ($[P]_{dynamic}$, $n = 8$) over time and as a function of BG content in the dynamic mode where 50% of the solution was exchanged regularly.

was measured at each time point and subsequently compared to the control SBF without any substrates. Comparing Figs. 4b and 5a, the change in [P] was much greater in the static mode, with the day 28 $[P]_{static}$ at a level almost twice that of the corresponding $[P]_{dynamic}$ ($p < 0.05$). While there was a steady decrease in [P] in the experimental group, solution [P] was significantly lower on day 28. The decrease in [P] in the static mode for the 50% BG group was significant over time ($p < 0.05$), while no temporal change was detected in [P] for the SBF control ($p > 0.05$).

A similar response was observed for the solution calcium concentration ([Ca]) in the static mode where the SBF was not exchanged every other day. As seen in Fig. 5b, solution [Ca] increased to 8 mM at day 1, and

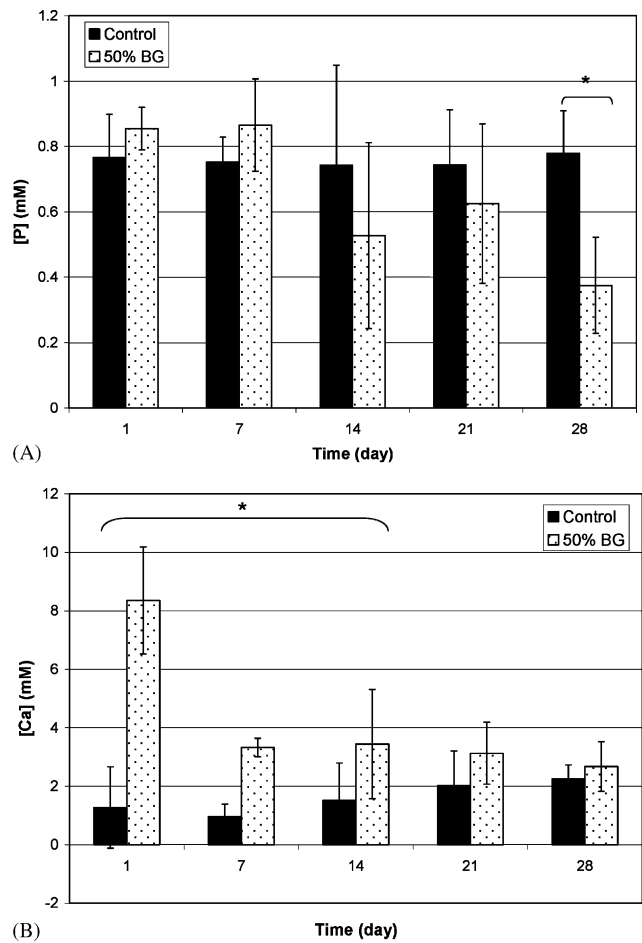


Fig. 5. Dissolution and precipitation of Ca and P during the formation of the calcium phosphate layer. A significant decrease in both Ca and P concentration were observed for the 50% BG group when the experiments were performed in the static mode where no solution was exchanged. The precipitation action of both Ca and P ions were more pronounced in the static mode compared to the dynamic mode where 50% of the solution was exchanged periodically. “*” denotes significance at $p < 0.05$. (a) Temporal solution phosphorus concentration ($[P]_{static}$, $n = 8$) compared to SBF control. (b) Temporal solution calcium concentration ($[Ca]_{static}$, $n = 8$) compared to control SBF.

decreased to about 3 mM at day 7, and remained relatively constant for the rest of the immersion period. The [Ca] in the PLAGA–BG composite was significantly higher at days 1 and 7 compared to the SBF control without any composite material. Similar to the case for [P] of SBF control, the slight fluctuations in solution [Ca] in the control SBF was not significant over time.

3.2. Compositional effects on the response of osteoblasts on PLAGA–BG composites

The effects of BG content on the growth of osteoblast-like cells on the PLAGA–BG composite are summarized in Fig. 6. Live/dead assay confirmed the viability of SaOS-2 cells on all substrates tested (data

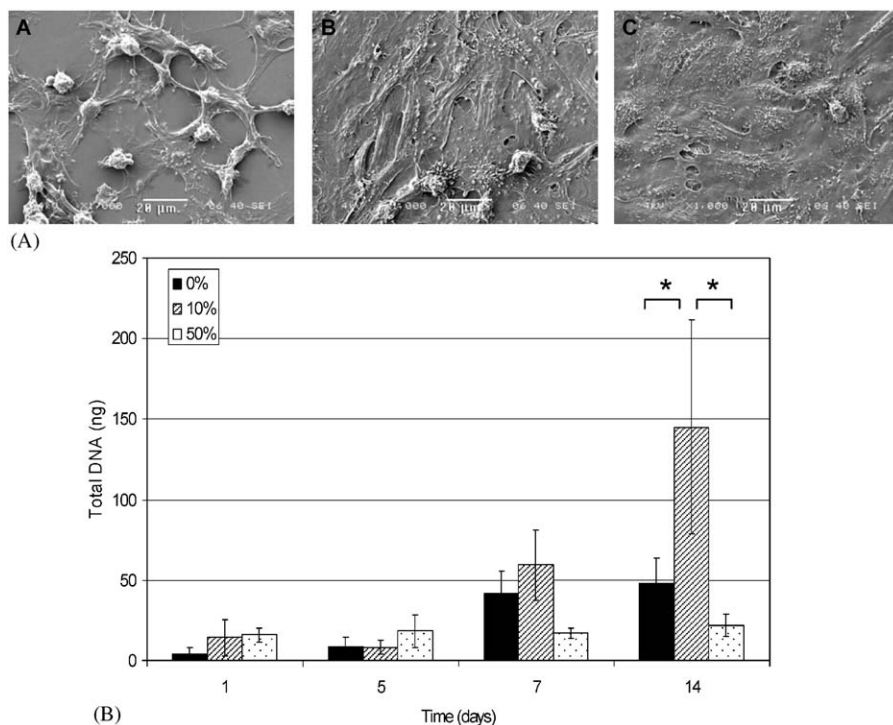


Fig. 6. Effects of composition on the growth of osteoblast-like cells on the polymer-bioactive glass composite (PLAGA–BG). SaOS-2 cells attached and grew on all substrates tested (Fig. 6A, A: 0%, B: 10%, C: 50% BG). The PLAGA–BG composite with 10% BG supported the highest level of cell proliferation compared to the control PLAGA (0% BG) and the 50% BG group ($p < 0.05$). These findings suggest that there may exist a threshold BG content which is optimal for osteoblast growth, and the interactions between PLAGA and BG at higher BG content may have an effect on cell proliferation. “*” denotes significance at $p < 0.05$. (a) Electron micrograph of cell growth morphology on 0% to 50% BG samples, $1000\times$. (b) The growth of SaOS-2 cells on 0–50% BG samples over time ($n = 6$).

not shown), and visually the cells formed confluent layers on the composite surfaces. As seen in Fig. 6a, SaOS-2 cells assumed spindle-shaped, osteoblast-like morphology on the samples. Significant matrix production was seen on the 0%, 10% and 50% BG composites after 14 days. The 10% BG supported the highest level of cell proliferation compared to the control PLAGA (0% BG) and the 50% BG group (Fig. 6b, $p < 0.05$). Cell growth on the PLAGA control plateaued after 1 week of culture. In contrast, the SaOS-2 cells continued to grow over time on the 10% BG group. Cell number was lower for the 50% group and remained relatively constant over the 2-week culturing period.

The effects of BG content on the differentiation of osteoblast-like cells on the PLAGA–BG composite are presented in Figs. 7 and 8. Qualitative assay of ALP activity (Fig. 7a) on the PLAGA and PLAGA–BG surfaces revealed that ALP activity was detectable and found to be abundant on both surfaces prior to the addition of mineralization media at day 7. As shown in Fig. 7b, quantitative ALP activity peaked at day 7 on the 10% BG composite, similar to what was reported for SaOS-2 monolayer controls [8]. In contrast, ALP activity was delayed on the 0% BG control and the highest level was measured on day 14. Relatively

minimal ALP activity was measured on the 50% BG group, and it was found to be significantly lower compared to the 0% group at day 14, and the 10% BG composite group at days 1, 7 and 14 ($p < 0.05$).

The effects of BG content on the mineralization of osteoblast-like cells grown on the PLAGA–BG composites are shown in Fig. 8. As seen in Fig. 8a, prior to the addition of the mineralization media, little or no mineralization and minimal staining was observed on the PLAGA control while, in contrast, uniform and homogeneous distribution of positive staining was observed on the 10% BG group. At day 28, all three groups of substrates examined (0%, 10%, 50%) stained positive for mineralization. As shown in Fig. 8b, the strongest staining intensity was observed in the 50% group, followed by the 10% group and then the 0% control. The observed mineralization on the 10% and 50% BG groups is likely the sum of both substrate-mediated and cell-mediated mineralization.

4. Discussion

We report here the optimization and in vitro characterization of the PLAGA–BG composite scaffold,

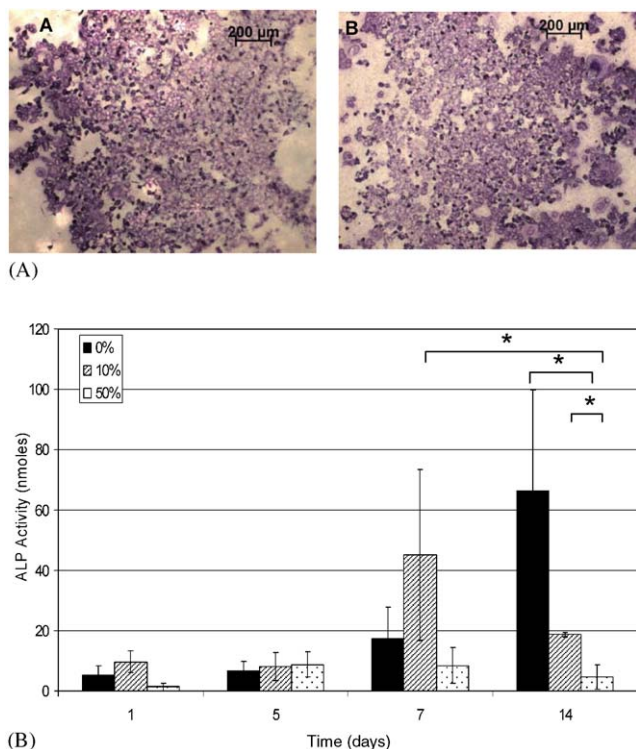


Fig. 7. Effects of composition on the differentiation of osteoblast-like cells on the polymer-bioactive glass composite (PLAGA–BG). ALP activity peaked on the 10% BG composite at day 7, similar to what was reported for SaOS-2 monolayer controls. In contrast, ALP activity was delayed on the 0% BG control and was found to be significantly lower on the 50% BG composite ($p < 0.05$). These observations suggest that the 10% BG composite may be more suitable for osteoblast differentiation compared to the 0% and 50% BG groups. “*” denotes significance at $p < 0.05$. (a) ALP activity on PLAGA–BG (A) and PLAGA (B) surfaces after 7 days of cell culture. (b) Quantitative ALP activity on PLAGA and PLAGA–BG substrates over time ($n = 6$).

with intended application as a bone tissue engineering scaffold or the bony phase of an interfacial graft. The objective of this study was to determine the effects of BG content on the kinetics of surface Ca–P layer formation, and to examine the temporal response of human osteoblast-like cells to the PLAGA–BG composite as a function of BG content. It was found that BG content had a significant effect on both the kinetics of Ca–P layer formation and the corresponding osteoblastic response.

The mechanisms underlying the formation of the Ca–P layer on PLAGA–BG composites are not yet well understood. It is likely that the series of ion dissolution and precipitation reactions described for 100% BG [19,21,33] also occur for the composite when it is exposed to an electrolyte solution. Characterization of the composite surface over time and as a function of BG content revealed that the degree of Ca–P formation on PLAGA–BG increased when BG content increased. Interestingly, the chemistry of the resultant Ca–P

surface was found to be also dependent on the BG content, as elemental composition varied between the 10%, 25% and 50% BG groups. FTIR analysis revealed that after 21 days of immersion, only the PLAGA–BG surface with 50% BG formed a crystalline Ca–P layer. These findings suggest that the kinetics of Ca–P layer formation is delayed in the composite system compared to the 100% BG surfaces.

It has been reported that the 100% BG surface forms an amorphous Ca–P layer after 1 day of immersion in SBF, and this surface is later transformed into a crystalline Ca–P layer after 3 days of immersion [19,21,33]. In contrast, for the PLAGA–BG composite, only the 50% BG group formed a crystalline Ca–P layer, and it was not detected by FTIR until after 2 weeks of immersion in SBF. Blaker et al. [34] reported on the formation of crystalline Ca–P on 5% PDLLA–BG foams within 3 days in SBF. Comparison to our study is limited since the immersion ratio was not given which will have a profound effect on the rate of Ca–P formation [19]. The characterization methods used found that the Ca–P development was heterogeneous on the 5% BG composite [34]. The comparative merit of an amorphous versus crystalline Ca–P layer in the osteointegration potential of the composite is not known and should be investigated further. EDAX analysis revealed that surface composition was dependent on the amount of BG present in the composite, with a greater release of Si and Na at the higher BG content. The contribution of the polymeric phase and the effects of polymer degradation on the formation of the Ca–P layer on the composite have not been reported. The observed disparity in Ca–P layer kinetics, composition and crystallinity as a function of BG content or the corresponding PLAGA content may be due to the polymeric phase and its degradation over time. The degradation of PLAGA may alter the dissolution of Si, P, Na, and Ca ions from the BG phase, and in turn affect the kinetics of Ca–P formation.

The reactions taking place on the PLAGA–BG composite surfaces which lead to the development of a Ca–P layer are reflected in the observed changes in [Ca] and [P]. Based on the release profiles for P, which is the rate-limiting ion for mineralization, there was an initial dissolution of phosphate from the BG phase, followed by its precipitation at day 7 for the 50% BG group and at day 24 for the 25% group. There was also an initial burst of Ca release from the substrate, followed by Ca precipitation as immersion continued. These observed changes in solution [P] and [Ca] corresponded to the results of Qiu et al. [35], who investigated the effects of filler composition on the bioactivity of individual microspheres formed from modified BG and polylactide. Solution concentrations of Si, Ca and P were measured and a filler content-dependent decrease was found in solution [Ca] and [P] at an immersion ratio of

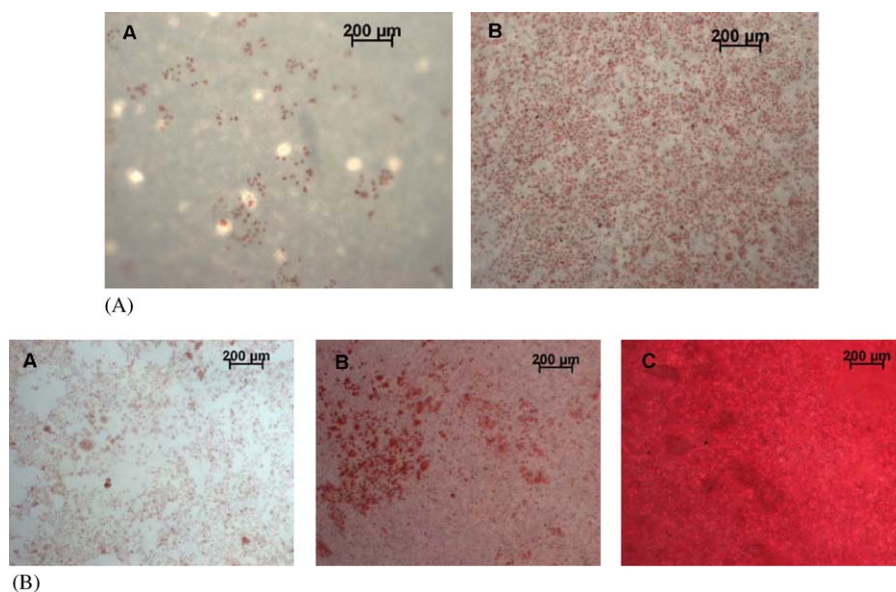


Fig. 8. Effects of composition on the mineralization of osteoblast-like cells on the polymer–bioactive glass composite (PLAGA–BG). Figs. 8A and B show Alizarin Red staining of substrates at days 7 and 28, respectively. While ALP activity was similar between 0% BG and 10% BG groups, the amount of mineralization was significantly higher on the 10% BG group, likely a combination of cell-mediated mineralization and surface Ca–P formation on the PLAGA–BG (Fig. 8A–B) composite. (A) Mineralization on PLAGA–BG and PLAGA–BG (Fig. 8A–A) surfaces after 7 days of culture. (B) Mineralization on sample surfaces (A: 0%, B: 10%, C: 50% BG) after 28 days of culture.

0.5 mg ml⁻¹ in the static mode. These results collectively suggest that the dissolution and precipitation of Ca and P are both involved in the formation of the Ca–P layer on the PLAGA–BG.

In this study, both the static and dynamic mode of immersion were investigated, as it had been previously reported that frequency of solution exchange had an effect on BG surface reactions [36]. In the static mode, no media exchange is performed, thus ion concentration values will eventually reach steady state. In the dynamic mode, fresh solution is added periodically to the system to emulate the local changes in ion concentration and utilization. The rationale here was to identify an optimal and realistic *in vitro* model that will mimic the local bone-grafting environment within which the composite will be situated. Continuous interstitial fluid exchange or infiltration of vasculature will alter the local concentration of the ions leached from the PLAGA–BG composite, as well as modify the availability of relevant ions involved in the mineralization process. Therefore, the temporal concentration and spatial distribution of ions within the graft site are expected to vary as a function of fluid infiltration during the initial repair response, as well as the subsequent uptake of relevant ions for Ca–P layer formation and cell mineralization during the bone regeneration stage. The aforementioned changes in [Ca] and [P] in the dynamic mode were enhanced when the concentration gradient was removed in the static mode. In other words, the decrease in ion concentration became more marked in the dynamic

mode. The dynamic mode also mimics the media exchange performed in the *in vitro* osteoblast experiments reported here. The observed changes in the Ca–P formation kinetics and composition in this study were related to surfaces developed in the dynamic mode, and may better simulate the *in vivo* environment.

In terms of osteoblast response to the composite surface as a function of BG content, it was found that the 10% BG substrates supported higher osteoblast growth and ALP activity compared to the PLAGA control (0% BG) and the 50% BG group. While ALP activity was similar between the 0% BG and 10% BG groups, the amount of mineralization was significantly higher on the 10% BG group, likely a combination of cell-mediated mineralization and surface Ca–P formation on the PLAGA–BG composite. The response of SaOS-2 cells to the 25% substrate was not investigated here as it was examined in a previous study [8]. It was found then that the 25% BG composite supported the growth, synthesis of type I collagen and mineralization by human osteoblast-like cells. Synthesis of type I collagen was found to be the highest on the polymer–BG composite as compared to PLAGA alone and tissue culture plastic controls. The decreased overall osteoblast response to the 50% BG surface was unexpected, as solution pH was within the physiological range and the osteoconductivity of the pre-treated 100% BG substrates had been well established in the literature [21,22,37,38]. A similar response was observed for chondrocytes grown on PLAGA–BG scaffolds [39],

where the 25% BG supported greater chondrocyte proliferation compared to the 0% or the 50% BG groups. Verrier et al. [40] reported a similar reduction in the rate of cell growth on PDLLA–BG foams with 40% BG. It is possible that interactions between PLAGA degradation products and ions released from BG during surface transformation may hinder cell growth. These results suggest that the polymer phase of the composite may play an important role in mediating cellular response to the composites, and its effects should be investigated further.

It is emphasized that the mineralization observed on the PLAGA–BG scaffolds *in vitro* is a combination of cell-mediated mineralization and the development of a mineralized matrix on the composites as a function of BG content. The strong positive staining seen on the 50% BG surface may be attributed to the increased bioactivity of the surface at the higher BG content, as cell growth was not found to be significant on the 50% BG composite. The kinetics of Ca–P layer formation and resultant chemistry were reported to be different for BG surfaces exposed to conditions with and without osteoblasts [37], and will be investigated in future studies with the 2-D and 3-D composite. In addition, the effects of BG content and porosity on PLAGA–BG scaffold mechanical properties and degradation rate will be examined in future studies.

5. Conclusions

In summary, the kinetics of Ca–P layer formation and the resulting Ca–P chemistry measured on the PLA–GA–BG composites were found to be dependent on BG content. The growth and differentiation of human osteoblast-like cells on the PLAGA–BG composite was also a function of BG content. The selection criteria for the optimal BG content for bone tissue engineering applications were based on the ability to form a surface Ca–P layer and to promote osteoblast growth and maturation over the 4-week culturing period. Based on the results of our studies, the 10% and 25% BG composite may be more suitable for osteoblast differentiation compared to the 50% BG group. The findings of this study suggest that there is a threshold BG content, which is optimal for osteoblast growth, and the interactions between PLAGA and BG may modulate the kinetics of Ca–P formation and the overall osteoblastic response.

Acknowledgement

The authors would like to gratefully acknowledge Dr. X. Edward Guo of Columbia University for assistance with micro-CT analyses and Dr. Steven Nicoll of the

University of Pennsylvania for providing the qualitative ALP staining protocol. This study was supported by the Whitaker Foundation Biomedical Engineering Research Grant RG-02-0004 (LuHH).

References

- [1] Langer R, Vacanti JP. Tissue engineering. *Science* 1993;260(5110):920–6.
- [2] Cook SD, Baffes GC, Wolfe MW, Sampath TK, Rueger DC, Whitecloud TS3. The effect of recombinant human osteogenic protein-1 on healing of large segmental bone defects. *J Bone Joint Surg Am* 1994;76(6):827–38.
- [3] Laurencin CT, Ambrosio AA, Borden M, Cooper JA. Tissue Engineering: Orthopedic Applications. In: Yarmush ML, Diller KR, Toner M, editors. *Annual Review of Biomedical Engineering*. 1999, p. 19–46.
- [4] Zhang R, Ma PX. Poly(alpha-hydroxyl acids)/hydroxyapatite porous composites for bone-tissue engineering. I. Preparation and morphology. *J Biomed Mater Res* 1999;44(4):446–55.
- [5] Mikos AG, Sarakinos G, Leite SM, Vacanti JP, Langer R. Laminated three-dimensional biodegradable foams for use in tissue engineering. *Biomaterials* 1993;14:323–30.
- [6] Agrawal CM, Ray RB. Biodegradable polymeric scaffolds for musculoskeletal tissue engineering. *J Biomed Mater Res* 2001;55(2):141–50.
- [7] Bonfield W, Grynblas MD, Tully AE, Bowman J, Abram J. Hydroxyapatite reinforced polyethylene—a mechanically compatible implant material for bone replacement. *Biomaterials* 1981;2(3):185–6.
- [8] Lu HH, El Amin SF, Scott KD, Laurencin CT. Three-dimensional, bioactive, biodegradable, polymer-bioactive glass composite scaffolds with improved mechanical properties support collagen synthesis and mineralization of human osteoblast-like cells *in vitro*. *J Biomed Mater Res* 2003;64A(3):465–74.
- [9] Niederauer GG, Cullen LC, Kieswetter K, Leatherbury NC, Walter MA, Greenspan DC, Shong JP, Boyan BD. Development of polylactide-co-glycolide/bioglass composites. *Soc Biomater Proc* 1997;23:162.
- [10] Qiu QQ, Ducheyne P, Ayyaswamy PS. New bioactive, degradable composite microspheres as tissue engineering substrates. *J Biomed Mater Res* 2000;52(1):66–76.
- [11] Marcolongo M, Ducheyne P, Garino J, Schepers E. Bioactive glass fiber/polymeric composites bond to bone tissue. *J Biomed Mater Res* 1998;39(1):161–70.
- [12] Roether JA, Boccaccini AR, Hench LL, Maquet V, Gautier S, Jerjme R. Development and *in vitro* characterisation of novel bioresorbable and bioactive composite materials based on polylactide foams and bioglass for tissue engineering applications. *Biomaterials* 2002;23(18):3871–8.
- [13] Zhang K, Wang Y, Hillmyer MA, Francis LF. Processing and properties of porous poly(L-lactide)/bioactive glass composites. *Biomaterials* 2004;25(13):2489–500.
- [14] Hench LL, Splinter RJ, Allen WC, Greenlee TK. Bonding mechanisms at the interface of ceramic prosthetic materials. *J Biomed Mater Res* 1971;2(Part1):117–41.
- [15] Hench LL, Paschall HA. Direct chemical bond of bioactive glass-ceramic materials to bone and muscle. *J Biomed Mater Res* 1973;4:25–42.
- [16] Bonfield W. Hydroxyapatite-reinforced polyethylene as an analogous material for bone replacement. *Ann NY Acad Sci* 1988;523:173–7.
- [17] Fujii T, Ogino M. Difference of bond bonding behavior among surface active glasses and sintered apatite. *J Biomed Mater Res* 1984;18(7):845–59.

- [18] Ducheyne P, Radin S, King L. The effect of calcium phosphate ceramic composition and structure on in vitro behavior. I. Dissolution. *J Biomed Mater Res* 1993;27(1):25–34.
- [19] Hench LL. Bioceramics: from concept to clinic. *J Am Cera Soc* 1991;74(7):1487–510.
- [20] Oonishi H. Orthopaedic applications of hydroxyapatite. *Biomaterials* 1991;12(2):171–8.
- [21] Ducheyne P. Bioceramics: material characteristics versus in vivo behavior. *J Biomed Mater Res* 1987;21:219–36.
- [22] Hench LL, Wilson J. Surface-active biomaterials. *Science* 1984;226:630–6.
- [23] Oonishi H, Kushitani S, Yasukawa E, Iwaki H, Hench LL, Wilson J, Tsuji E, Sugihara T. Particulate bioglass compared with hydroxyapatite as a bone graft substitute. *Clin Orthop* 1997(334):316–25.
- [24] Davies JE, Baldan N. Scanning electron microscopy of the bone-bioactive implant interface. *J Biomed Mater Res* 1997;36(4):429–40.
- [25] Gatti AM, Valdre G, Andersson OH. Analysis of the in vivo reactions of a bioactive glass in soft and hard tissue. *Biomaterials* 1994;15:208–12.
- [26] Schepers E, de Clercq M, Ducheyne P, Kempeneers R. Bioactive glass particulate material as a filler for bone lesions. *J Oral Rehabil* 1991;18(5):439–52.
- [27] Yaszemski MJ, Payne RG, Hayes WC, Langer R, Mikos AG. Evolution of bone transplantation: molecular, cellular and tissue strategies to engineer human bone. [Review] [74 refs]. *Biomaterials* 1996;17(2):175–85.
- [28] Habal MB, Reddi AH. Bone grafts and bone induction substitutes. [Review]. *Clin Plastic Surg* 1994;21:525–42.
- [29] Lu HH, Pollack SR, Ducheyne P. Temporal zeta potential variations of 45S5 bioactive glass immersed in an electrolyte solution. *J Biomed Mater Res* 2000;51(1):80–7.
- [30] Lin AS, Barrows TH, Cartmell SH, Guldborg RE. Microarchitectural and mechanical characterization of oriented porous polymer scaffolds. *Biomaterials* 2003;24(3):481–9.
- [31] Heinonen JK, Lahti RJ. A new and convenient colorimetric determination of inorganic orthophosphate and its application to the assay of inorganic pyrophosphatase. *Anal Biochem* 1981;113(2):313–7.
- [32] Murphy WL, Kohn DH, Mooney DJ. Growth of continuous bonelike mineral within porous poly(lactide-co-glycolide) scaffolds in vitro. *J Biomed Mater Res* 2000;50(1):50–8.
- [33] Kokubo T. Bioactivity of glasses and glass ceramics. In: Ducheyne P, Kokubo T, van Blitterswijk, editors. *Bone-bonding-Reed Healthcare Communications*. 1992, p. 31–46.
- [34] Blaker JJ, Gough JE, Maquet V, Notingher I, Boccaccini AR. In vitro evaluation of novel bioactive composites based on Bioglass-filled polylactide foams for bone tissue engineering scaffolds. *J Biomed Mater Res A* 2003;67(4):1401–11.
- [35] Qiu QQ, Ducheyne P, Ayyaswamy PS. Bioactive, degradable composite microspheres: effect of filler material on surface reactivity. *Ann N Y Acad Sci* 2002;974:556–64.
- [36] Radin S, Falaize S, Lee MH, Ducheyne P. In vitro bioactivity and degradation behavior of silica xerogels intended as controlled release materials. *Biomaterials* 2002;23(15):3113–22.
- [37] El Ghannam AR, Ducheyne P, Shapiro IM. Bioactive material template for in vitro synthesis of bone. *J Biomed Mater Res* 1995;29(3):359–70.
- [38] Kaufmann EA, Ducheyne P, Shapiro IM. Effect of varying physical properties of porous, surface modified bioactive glass 45S5 on osteoblast proliferation and maturation. *J Biomed Mater Res* 2000;52(4):783–96.
- [39] Lu HH, Jiang J, Tang A, Hung CT, Guo XE. Development of controlled heterogeneity on a polymer-ceramic hydrogel scaffold for osteochondral repair. *Bioceramics* 2005;17(Key Engineering Materials Vols. 284–286):607–10.
- [40] Verrier S, Blaker JJ, Maquet V, Hench LL, Boccaccini AR. PDLA/Bioglass composites for soft-tissue and hard-tissue engineering: an in vitro cell biology assessment. *Biomaterials* 2004;25(15):3013–21.